Effect of solvent on reactions of $Cp_2Zr\{(\mu\text{-}H)_2BHR\}_2$ and $Cp_2ZrH\{(\mu\text{-}H)_2BHR\}$ (R = CH$_3$, Ph) with $B(C_6F_5)_3$

Fu-Chen Liu [a,*], Shou-Chon Chen [a], Gene-Hsian Lee [b], Shie-Ming Peng [b]

[a] *Department of Chemistry, National Dong Hwa University, Hualien 974, Taiwan, ROC*
[b] *Department of Chemistry, National Taiwan University, Taipei 106, Taiwan, ROC*

Abstract

The effect that a solvent has on reactions of $Cp_2Zr\{(\mu\text{-}H)_2BHR\}_2$ and $Cp_2ZrH\{(\mu\text{-}H)_2BHR\}$ (R = CH$_3$, Ph) with $B(C_6F_5)_3$ has been studied. From the reaction in benzene the metathesis product $Cp_2Zr\{(\mu\text{-}H)_2B(C_6F_5)_2\}_2$, **2**, was isolated. In the case of diethyl ether, different hydride abstraction products, including $[Cp_2Zr(OEt_2)\{(\mu\text{-}H)_2BHPh\}][HB(C_6F_5)_3]$, **3**, $[Cp_2Zr(OEt_2)\{(\mu\text{-}H)_2BHCH_3\}][HB(C_6F_5)_3]$, **4**, $[Cp_2Zr(OEt_2)\{(\mu\text{-}H)_2BH_2\}][HB(C_6F_5)_3]$, **5**, and $[Cp_2Zr(OEt)(OEt_2)][HB(C_6F_5)_3]$, **6**, were isolated depending on the starting zirconocene complex. The diethyl ether molecules of **3–6** are weakly coordinated to Zr and displaced in THF solution. Isolation of **3** and **4** is attributed to their fast precipitation from the reaction mixture, which prevented further reactions from occurring. In addition to the hydride abstraction, a hydride metathesis was also involved in the formation of **5**. Time-elapsed ^{11}B NMR studies indicate that **3** and **4** are the intermediates on the pathway to **5** and **6**. The molecular structures of **2–6** were determined by single-crystal X-ray diffraction.
© 2007 Elsevier B.V. All rights reserved.

Keywords: Organotrihydroborate; Metathesis; Hydride abstraction

1. Introduction

Recently there has been an increased interest in the preparation of metallocene cations of the $[Cp_2'MR]^+$ type (Cp$'$ = C$_5$H$_5$, C$_5$Me$_5$; M = Zr, Ti), due to their catalytic activity in Ziegler–Natta olefin polymerization [1]. Although in rare cases these 14e$^-$ cationic species have been isolated, preparation of THF adducts of ionic compounds $[Cp_2'MR]^+[X]^-$ (X = BPh$_4$, BR(C$_6$F$_5$)$_3$) is much more common [2]. The catalytic ability of $[Cp_2ZrR(THF)]^+$ has been studied [3]. In addition to the alkyl carbanion abstraction to form a cation, the Lewis acid $B(C_6F_5)_3$ can also abstract a terminal hydride from a metallocene hydride or a bridging hydrogen M–H–B from a metallocene organohydroborate complex. Marks and co-workers showed that abstraction of a hydride from $Cp_2^*ZrH_2$ by $B(C_6F_5)_3$ results in the ionic compound $[Cp_2^*ZrH][HB(C_6F_5)_3]$ [4]. Several examples of hydride abstraction from metallocene cyclic organodihydroborates using $B(C_6F_5)_3$ have been reported by Shore and co-workers. These reactions have been shown to be solvent-dependent, with different products being isolated from non-coordinating and coordinating solvents. In the case of toluene, a non-coordinating solvent, $B(C_6F_5)_3$ removed the hydride from $Cp_2ZrH\{(\mu\text{-}H)_2BR\}$ (R = C$_4$H$_8$, C$_5$H$_{10}$) yielding a single hydrogen-bridged compound $[(\mu\text{-}H)\{Cp_2Zr(\mu\text{-}H)_2BR\}_2][HB(C_6F_5)_3]$. From diethyl ether, a coordinating solvent, the ethoxy-substituted compound $[Cp_2Zr(OEt_2)(OEt)][HB(C_6F_5)_3]$ was isolated [5]. On the other hand, reactions of titanium compounds $Cp_2Ti\{(\mu\text{-}H)_2BR\}$ (R = C$_4$H$_8$, C$_5$H$_{10}$, C$_8$H$_{14}$) with $B(C_6F_5)_3$ furnished a metathesis product $Cp_2Ti\{(\mu\text{-}H)_2B(C_6F_5)_2\}$ in toluene and the ionic compound $[Cp_2Ti(OEt_2)_2][HB(C_6F_5)_3]$ in ether [6]. A more complicated result was obtained when $Cp_2Nb\{(\mu\text{-}H)_2BR\}$ (R = C$_4$H$_8$, C$_5$H$_{10}$, C$_8$H$_{14}$) was reacted

---

* Corresponding author. Tel.: +886 3 8633601; fax: +886 3 8633570.
E-mail address: fcliu@mail.ndhu.edu.tw (F.-C. Liu).

with $B(C_6F_5)_3$. In toluene the ionic compound $[Cp_2Nb(\mu\text{-}H)(\eta^5\text{-}\eta^1\text{-}C_5H_4)Nb(\eta^5\text{-}\eta^1\text{-}C_5H_4)_2Nb\{(\mu\text{-}H)(\eta^5\text{-}\eta^1\text{-}C_5H_4B\text{-}(C_6F_5)_2)\}][HB(C_6F_5)_3]$ formed, however, the neutral compound $CpNb(B(C_6F_5)\{(\mu\text{-}H)(\eta^5\text{-}C_5H_4B(C_6F_5)_2)\})$ was obtained from the reaction in ether [7]. It has been reported in our recent study that several group 4 metallocene organotrihydroborate compounds display properties different from those of their cyclic organodihydroborate analogs [8]. For the purpose of further comparison of the metallocene organodihydroborate and the organotrihydroborate complexes, we were interested in reactions of complexes of the latter type with $B(C_6F_5)_3$. In this contribution, we report on the recent results obtained from the studies of reactions of $Cp_2Zr\{(\mu\text{-}H)_2BHR\}_2$ and $Cp_2ZrH\{(\mu\text{-}H)_2BHR\}$ (R = CH_3, Ph) with $B(C_6F_5)_3$ in both benzene and diethyl ether.

2. Results and discussion

2.1. Formation and properties of $Cp_2ZrH\{(\mu\text{-}H)_2BHCH_3\}$ (1), $Cp_2Zr\{(\mu\text{-}H)_2B(C_6F_5)_2\}_2$ (2), $[Cp_2Zr(OEt_2)\{(\mu\text{-}H)_2BHPh\}][HB(C_6F_5)_3]$ (3), $[Cp_2Zr(OEt_2)\{(\mu\text{-}H)_2BHCH_3\}][HB(C_6F_5)_3]$ (4), $[Cp_2Zr(OEt_2)\{(\mu\text{-}H)_2BH_2\}][HB(C_6F_5)_3]$ (5), and $[Cp_2Zr(OEt)(OEt_2)][HB(C_6F_5)_3]$ (6)

Previously compound $Cp_2ZrH\{(\mu\text{-}H)_2BHCH_3\}$, **1**, has been prepared in low yield through the reaction of Cp_2ZrCl_2 with excess amount of $LiBH_3CH_3$ followed by sublimation [9]. NMR studies from our group have shown that **1** is a product of $Cp_2Zr\{(\mu\text{-}H)_2BHCH_3\}_2$ decomposition [8], however, it is not practical to use this as a method for a large scale preparation of **1**. Thus, compound **1** was prepared from the reaction of $Cp_2Zr\{(\mu\text{-}H)_2BHCH_3\}_2$ with $N(C_2H_5)_3$ in ether according to Eq. (1). The ease of the by-product $CH_3BH_2 \cdot N(C_2H_5)_3$ removal under a dynamic vacuum and the high isolated yield of **1** are the distinct advantages of this method.
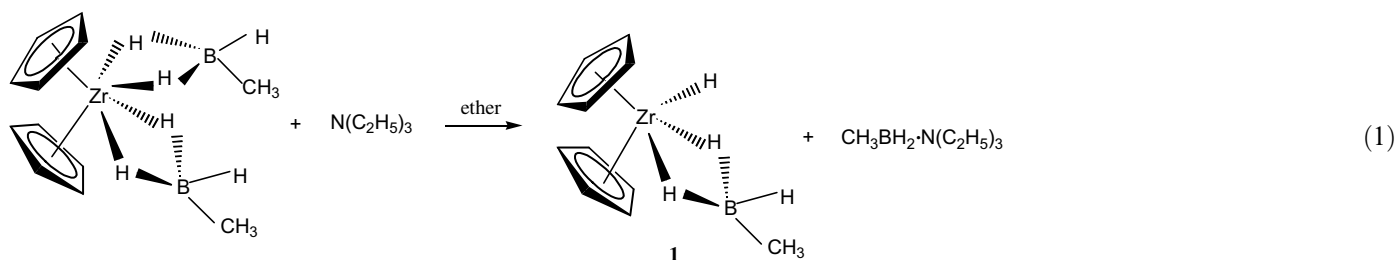
The reactions of either $Cp_2Zr\{(\mu\text{-}H)_2BHR\}_2$ or $Cp_2ZrH\{(\mu\text{-}H)_2BHR\}$ (R = CH_3, Ph) with $B(C_6F_5)_3$ in benzene yielded compound $Cp_2Zr\{(\mu\text{-}H)_2B(C_6F_5)_2\}_2$, **2** according to Scheme 1. Two equivalents of $B(C_6F_5)_3$ were used in the case of *bis*(organohydroborate) compounds $Cp_2Zr\{(\mu\text{-}H)_2BHR\}_2$, however, 3 equiv. of $B(C_6F_5)_3$ were

required in the case of zirconium hydride compounds $Cp_2ZrH\{(\mu\text{-}H)_2BHR\}$. Under these conditions, **2** is a major product along with several unidentified species, which are soluble in benzene and characterized by singlet signals in ^{11}B NMR. Compound **2** has been previously prepared by Piers and co-workers [10] from the reaction of $Cp_2Zr(CH_3)_2$ with $HB(C_6F_5)_2$ in benzene. Overall, our data obtained for **2** are consistent with those reported by Piers, except for the IR data displaying an additional strong absorption band at 1475 cm^{-1} in KBr compared with the literature spectrum acquired in Nujol. This discrepancy could be explained taking into account that Nujol itself has a strong broad absorption band at 1460 cm^{-1}.

Competing reactions took place when $Cp_2Zr\{(\mu\text{-}H)_2BHR\}_2$ and $Cp_2ZrH\{(\mu\text{-}H)_2BHR\}$ (R = CH_3, Ph) were mixed with $B(C_6F_5)_3$ in diethyl ether. $[Cp_2Zr(OEt_2)\{(\mu\text{-}H)_2BHPh\}][HB(C_6F_5)_3]$, **3**, $[Cp_2Zr(OEt_2)\{(\mu\text{-}H)_2BHCH_3\}][HB(C_6F_5)_3]$, **4**, $[Cp_2Zr(OEt_2)\{(\mu\text{-}H)_2BH_2\}][HB(C_6F_5)_3]$, **5**, and $[Cp_2Zr(OEt)(OEt_2)][HB(C_6F_5)_3]$, **6**, were the major products resulting from the hydride abstraction (Scheme 2). Thus, $B(C_6F_5)_3$ removed the terminal hydride from $Cp_2ZrH\{(\mu\text{-}H)_2BHPh\}$ producing compound **3** (path a). A similar product, compound **4**, was isolated according to path b. In contrast, reactions of $Cp_2Zr\{(\mu\text{-}H)_2BHPh\}_2$ and $Cp_2ZrH\{(\mu\text{-}H)_2BHCH_3\}$ with $B(C_6F_5)_3$ produced compounds **5** (path c) and **6** (path d), respectively. Compound **6**, which is also a major by-product of reactions shown in paths a–c, can be isolated from reactions of $Cp_2Zr(\mu\text{-}H)_2BHR\}_2$ (R = CH_3, Ph) and $Cp_2ZrH(\mu\text{-}H)_2BHPh\}$ with two-fold excess of $B(C_6F_5)_3$ in diethyl ether, as described in the experimental section. The role of excess $B(C_6F_5)_3$ is to accelerate the formation of **6**, since compound **6** becomes a major product of reactions shown in paths **a** and **b** at prolonged stirring. These cationic species were isolated using crystallization. Crystals of **3** and **4** are slightly soluble in ether; however, those of **5** and **6** are practically insoluble.

$$\text{(1)}$$

The reactions of either $Cp_2Zr\{(\mu\text{-}H)_2BHR\}_2$ or $Cp_2ZrH\{(\mu\text{-}H)_2BHR\}$ (R = CH_3, Ph) with $B(C_6F_5)_3$ in

Using d_8-THF as a solvent to acquire the ^1H NMR spectra of compounds **3–5** resulted in displacement of the coordinated ether molecules by those of the deuterated solvent. Two broad signals corresponding to the hydrogens on boron atoms were observed. Thus, the terminal hydrogen of the anion appeared at 3.74 ppm for each compound,
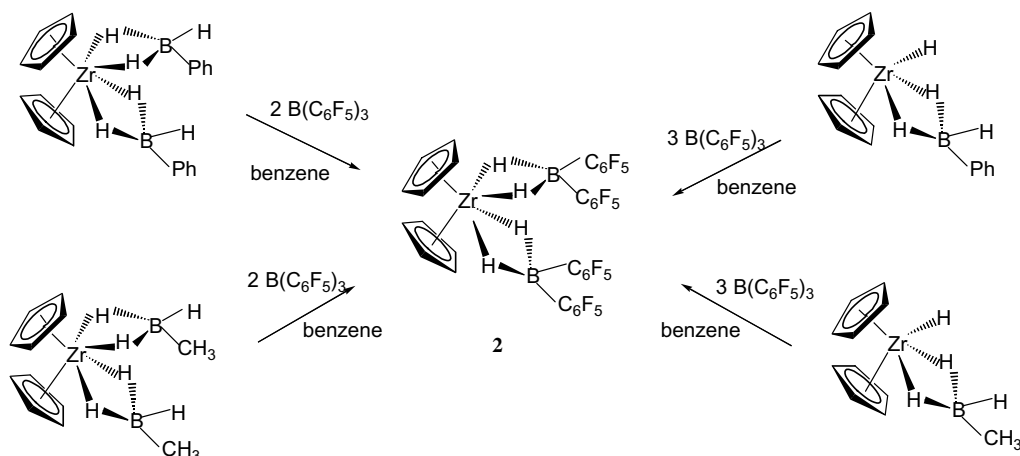
Scheme 1.
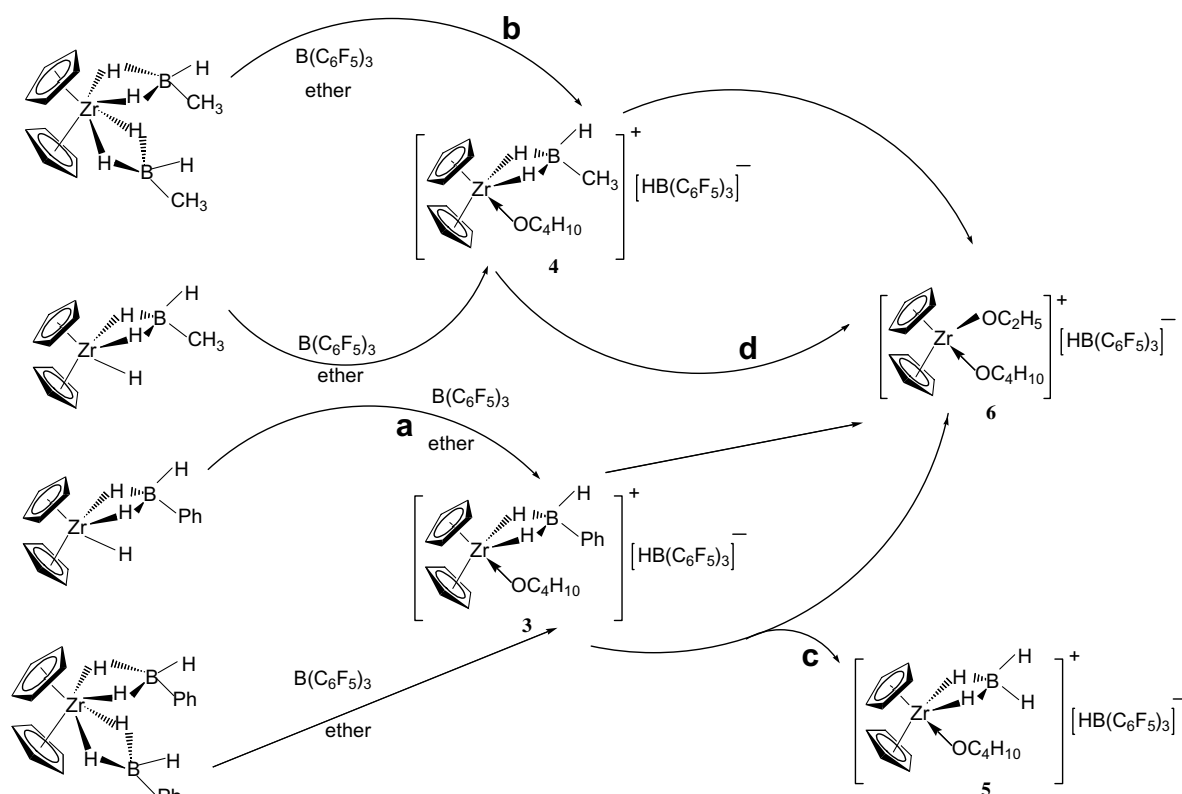
Scheme 2.

as previously reported for **6** [5a]. In contrast, for the cationic part the chemical shift depends on the substituent on the boron atom. Thus, the cationic borohydride signals for **3**–**5** appear at 1.20, 0.65, and 0.85 ppm, respectively. Due to the fast exchange of bridging and terminal hydrogen atoms on the NMR timescale, only one cationic borohydride signal was observed for each complex. Two boron signals, a broad quartet and a doublet, were observed in the ^{11}B NMR spectra of **3**–**5**. The doublet appearing at about −26 ppm ($J_{B-H} = 93$ Hz) was assigned to the anion

$[HB(C_6F_5)_3]^-$. The boron chemical shifts of cations of **3**–**5** and their THF coordinated analogs are listed in Table 1. The chemical shifts of $[Cp_2Zr(OEt_2)\{(\mu\text{-}H)_2BH_2\}]^+$ was recorded during the reaction. In THF the coordinated ether was replaced by THF resulting in $[Cp_2Zr(THF)\{(\mu\text{-}H)_2BHR\}]^+$ cations. Although a boron chemical shift could differ slightly from one solvent to another, Table 1 indicates that all of the THF-coordinated compounds display upfield chemical shifts compared with their ether-coordinated counterparts. Since THF is a stronger electron

Table 1
The boron chemical shift (ppm) of the cation in (3)–(5) and their THF coordinated analogs

	$[Cp_2Zr(OEt_2)\{(\mu\text{-}H)_2BHR\}]^+$ in ether	$[Cp_2Zr(THF)\{(\mu\text{-}H)_2BHR\}]^+$ in THF
R = Ph (3)	13.75	11.90
R = CH$_3$ (4)	15.77	13.34
R = H (5)	4.33	2.08

Fig. 1. Molecular structure of $Cp_2Zr\{(\mu\text{-}H)_2B(C_6F_5)_2\} \cdot OC_4H_{10}$ showing 30% probability thermal ellipsoids.

donor than ether, it provides more electron density to the metal. Thus, the electron deficiency of the metal is alleviated resulting in the increased electron density on the boron atom and an upfield boron chemical shift.

Formation of **5** involves both a hydride abstraction and a hydride metathesis reaction. The time-elapsed ^{11}B NMR study of the reaction of $Cp_2Zr\{(\mu\text{-}H)_2BHPh\}_2$ with $B(C_6F_5)_3$ (Supplementary material Fig. S5) suggests compound **3** is the intermediate of the reaction. As time elapsed, colorless crystals of $[Cp_2Zr(OEt_2)\{(\mu\text{-}H)_2BH_2\}]$-$[HB(C_6F_5)_3]$ began to form while compound **3** gradually disappeared. The reaction occurred in a stepwise fashion. In the first step, $Cp_2Zr\{(\mu\text{-}H)_2BHPh\}_2$ reacted with $B(C_6F_5)_3$ to produce compound **3** and the organodiborane "$(BH_2Ph)_2$". Consequent metathesis reaction of this organodiborane or a product related to it with compound **3** produced compound **5** and triphenylborane $B(C_6H_5)_3$. Formation of **5** is unique as the outcome of this type has never been observed in reactions of $B(C_6F_5)_3$ with other organohydroborate complexes. In contrast, the reverse process, alkyl metathesis, has been reported by Schlesinger [11] and Marks [12] in their preparations of organohydroborate uranium complexes.

Compound **6** has been prepared from the reaction of $Cp_2ZrH\{(\mu\text{-}H)_2BR\}$ (R = C_4H_8, C_5H_{10}) with $B(C_6F_5)_3$ [5]. A mechanism has been proposed for this reaction [13], however, no detailed NMR study has been performed. The time-elapsed ^{11}B NMR study of the reaction of $Cp_2ZrH\{(\mu\text{-}H)_2BHCH_3\}$ with $B(C_6F_5)_3$ (Supplementary material Fig. S6) suggests compound **4** is an intermediate in this reaction. Compound **4** formed in the beginning of the reaction. As time elapsed, compound **4** disappeared and crystals of compound **6** formed gradually inside the NMR tube. This result confirms the mechanism proposed previously [13].

The time-elapsed ^{11}B NMR studies suggest that compounds **3** and **4** are intermediates on the pathway to **5** and **6**. The key point to their successful isolation from reactions illustrated in Scheme 2 is their fast precipitation from the reaction mixtures, which prevents further reactions from occurring. However, under the conditions of reactions illustrated in paths c and d, compounds **3** and **4** did not precipitated immediately as they were forming, thus providing an opportunity for isolation of **5** and **6** due to further transformations.
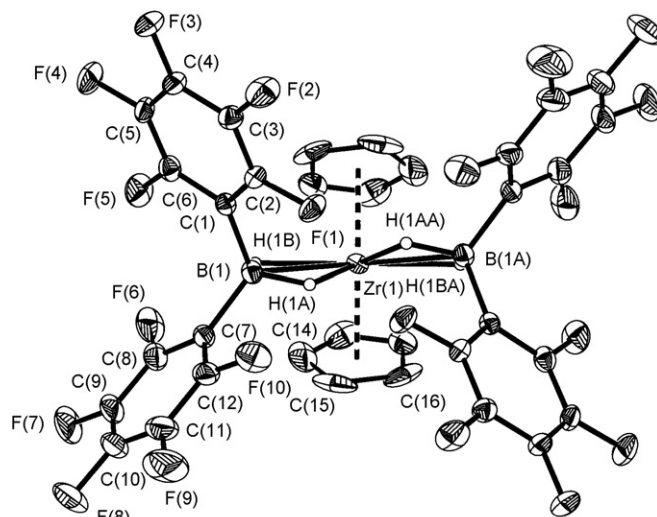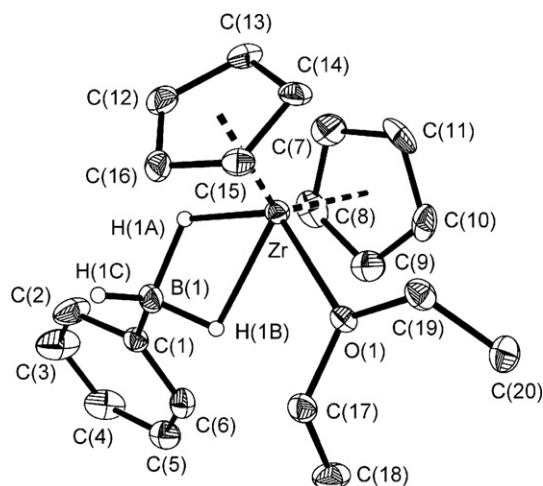
2.2. Molecular structures

The molecular structures of **2**–**6** were determined by single-crystal X-ray diffraction analysis. The crystals of **2** isolated from an ether solution contain the solvent of crystallization. The cell parameters obtained for **2** are slightly different from those reported by Piers and co-workers [10a] for the compound isolated from a benzene solution. Two molecules of **2** with slightly different bond distances and angles were found in the unit cell, and one of them is shown in Fig. 1. Comparison of their bond distances and angles with those for **2** isolated from benzene is presented in Table 2. Although the Zr–B distances (2.652(3) and 2.658(3) Å) for **2** isolated in this work are slightly shorter than that reported in literature (2.696(10) and 2.679(10) Å) [10a], compound **2** still has the longest reported Zr–H–B bond distance. Zr–H and B–H distances as well as the related bond angles reported here are more precise due to the fact that it was possible to locate and refine the bridging hydrogens of **2**.

The molecular structures of cations of compounds **3**–**5** are shown in Figs. 2–4. The corresponding crystallographic data, selected bond distances and bond angles are given in Tables 3–6. The molecular structure of **6** has been reported [5], the crystallographic data are included in the Supplementary material. The coordination geometries around zirconium atoms of **3**–**5** are the same and can be described best as distorted tetrahedrons. At the corners of a tetrahedron are the centers of two Cp rings, an oxygen atom, and a boron atom connected to the zirconium atom through two bridging hydrogens. For compound **4** two independent molecules were found in the unit cell. These two molecules have slightly different bond distances and angles, and only one molecular structure is presented. The hydrogens bound to the boron atoms were located and refined isotropically. The Zr–B distances are 2.561(5) Å in **3**, 2.514(12) and
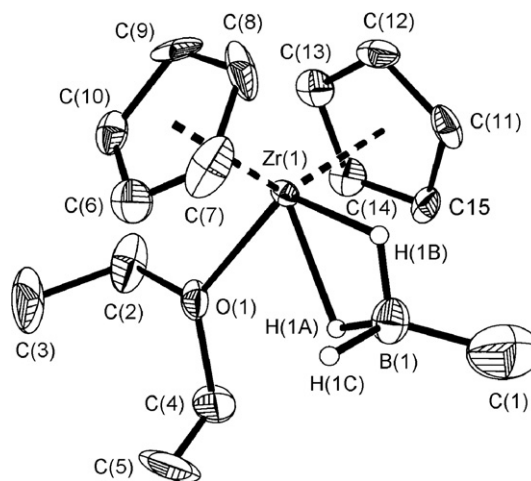
Table 2
Selected interatomic distances (Å) and bond angles (°) for Cp$_2$Zr{(μ-H)$_2$B(C$_6$F$_5$)$_2$}$_2$ · C$_6$H$_6$ and Cp$_2$Zr{(μ-H)$_2$B(C$_6$F$_5$)$_2$}$_2$ · OC$_4$H$_{10}$ (2)

| | Cp$_2$Zr{(μ-H)$_2$-B(C$_6$F$_5$)$_2$}$_2$ · C$_6$H$_6$[a] | Cp$_2$Zr{(μ-H)$_2$-B(C$_6$F$_5$)$_2$}$_2$ · OC$_4$H$_{10}$ | |
		(2′)	(2″)
Zr–H$_{bridge}$	2.043	2.12(2)	2.12(2)
	2.054	2.12(2)	2.14(2)
	2.177		
	1.991		
B–H$_{bridge}$	1.234	1.19(2)	1.17(2)
	1.193	1.17(2)	1.13(2)
	1.295		
	1.243		
Zr–B	2.696(10)	2.652(3)	2.658(3)
	2.679(10)		
B(1)–C(7)	1.63(1)	1.620(3)	1.607(3)
	1.60(1)	1.608(4)	1.611(4)
	1.61(1)		
	1.62(1)		
H$_{bridge}$–Zr–H$_{bridge}$	50.30	51.2(9)	49.3(9)
	54.19		
H$_{bridge}$–B–H$_{bridge}$	91.65	101.9(17)	101.8(17)
	97.32		
C(1)–B(1)–C(7)	113.5(7)	112.4(2)	112.6(2)
	113.2(7)		

[a] From Ref. [10a].

Fig. 2. Molecular structure of the cation in [Cp$_2$Zr(OEt$_2$){(μ-H)$_2$BHPh}][HB(C$_6$F$_5$)$_3$] (3), showing 30% probability thermal ellipsoids.

Fig. 3. Molecular structure of the cation in [Cp$_2$Zr(OEt$_2$){(μ-H)$_2$BHCH$_3$}][HB(C$_6$F$_5$)$_3$] (4), showing 30% probability thermal ellipsoids.
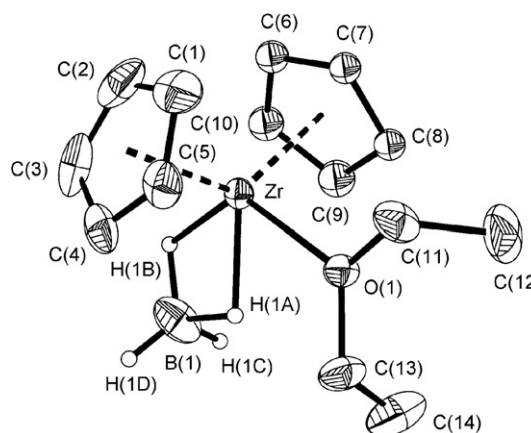
Fig. 4. Molecular structure of the cation in [Cp$_2$Zr(OEt$_2$){(μ-H)$_2$BH$_2$}][HB(C$_6$F$_5$)$_3$] (5), showing 30% probability thermal ellipsoids.

2.575(12) Å in 4, and 2.531(13) Å in 5. Compared with the Zr–B distances of the neutral alkylborate complexes found in the range of 2.538–2.696 Å [8,14], these cationic Zr–B distances are either shorter than, or falling into the above range for neutral compounds closer to its lower limit. The cationic character alone can not account for these short distances. Although the average Zr–B distance found in 4 is shorter than that found in Cp$_2$ZrH{(μ-H)$_2$BHCH$_3$} (2.558(4) Å) [9], the Zr–B distance in 3 is longer than that found in the corresponding zirconium hydride Cp$_2$ZrH{(μ-H)$_2$BHPh} (2.538(11) Å) [14]. Indeed, the steric effect also have to be considered. The cation

[(C$_5$H$_4$Me)$_2$Zr(THF){(μ-H)$_2$BH$_2$}]$^+$ (2.54(1) Å, 2.55(1) Å) [15] is more crowded than that in 5 and displays a longer Zr–B distance. The Zr–O distances are 2.263(3) Å in 3, 2.243(5) and 2.261(5) Å in 4, and 2.253(5) Å in 5. These Zr–O distances are longer than those found in [Cp$_2$Zr(CH$_3$)(THF)]$^+$ (2.122(14) Å) [16], [(C$_5$H$_4$Me)$_2$-Zr(THF){(μ-H)$_2$BH$_2$}]$^+$ (2.239(5), 2.231(6) Å) [15], [Cp$_2$Zr(OBu^t)(THF)]$^+$ (2.200(4) Å) [17], [Cp$_2$ZrCl(OEt$_2$)]$^+$ (2.211(3) Å) [14], [Cp$_2$Zr(OEt)(OEt$_2$)]$^+$ (2.209(8) Å) [5a], and the sum of the corresponding covalent radii (2.16 Å) [18]. This result is consistent with a weak coordinating ability of ether observed in the NMR study, where THF was found to be capable of displacing all coordinated ether molecules from the Zr inner coordination sphere. In these ether-coordinated cations, the ether ligand is oriented almost in the plane defined by boron, zirconium and oxygen atom of the ether molecule. The C–O–C angles of the ether ligand are similar to each other and falling in the range of 112.1–113.0°.

Table 3
Crystallographic data for $Cp_2Zr\{(\mu-H)_2B(C_6F_5)_2\}_2 \cdot OC_4H_{10}$ (2), $[Cp_2Zr(OEt_2)\{(\mu-H)_2BHPh\}][HB(C_6F_5)_3]$ (3), $[Cp_2Zr(OEt_2)\{(\mu-H)_2-BHCH_3\}][HB(C_6F_5)_3]$ (4), and $[Cp_2Zr(OEt_2)\{(\mu-H)_2BH_2\}][HB(C_6F_5)_3]$ (5)

Empirical formula	$C_{38}H_{24}B_2F_{20}OZr$	$C_{38}H_{29}B_2F_{15}OZr$	$C_{33}H_{27}B_2F_{15}OZr$	$C_{32}H_{25}B_2F_{15}Ozr$
Fw	989.41	899.45	837.39	823.36
T (K)	150(1)	150(1)	150(1)	150(1)
Crystal system	Monoclinic	Monoclinic	Triclinic	Monoclinic
Space group	$C2/c$	$P2_1/c$	$P\bar{1}$	$P2_1/n$
a (Å)	23.0148(12)	11.8403(5)	12.7385(6)	12.6640(5)
b (Å)	17.9319(9)	13.0180(6)	12.8112(5)	20.7530(8)
c (Å)	20.7311(10)	23.8777(10)	20.6137(8)	12.8779(5)
α (°)			91.360(1)	
β (°)	114.033(1)	95.873(1)	91.497(1)	104.117(1)
γ (°)			102.673(1)	
V (Å^3)	7814.0(7)	3661.1(3)	3279.5(2)	3282.3(2)
Z	8	4	4	4
ρ_{calcd} (g/cm^3)	1.682	1.632	1.696	1.666
Crystal size (mm)	$0.40 \times 0.40 \times 0.30$	$0.25 \times 0.20 \times 0.20$	$0.12 \times 0.10 \times 0.10$	$0.25 \times 0.10 \times 0.10$
Radiation (λ, Å)	Mo Kα (0.71073)	Mo Kα (0.71073)	Mo Kα (0.71073)	Mo Kα (0.71073)
2θ Limits (°)	1.49–27.50	1.71–27.50	0.99–25.00	1.90–25.00
Index ranges	$-29 \leqslant h \leqslant 29$,	$-15 \leqslant h \leqslant 15$,	$-15 \leqslant h \leqslant 15$,	$-15 \leqslant h \leqslant 15$,
	$-23 \leqslant k \leqslant 23$,	$-16 \leqslant k \leqslant 16$,	$-15 \leqslant k \leqslant 15$,	$-23 \leqslant k \leqslant 24$,
	$-19 \leqslant l \leqslant 26$	$-31 \leqslant l \leqslant 30$	$-24 \leqslant l \leqslant 24$	$-15 \leqslant l \leqslant 15$
Reflections collected	31341	35145	29441	26618
Unique reflections	8970	8397	11543	5769
Unique reflections [$I > 2.0\sigma(I)$]	3920	1800	1672	1640
Completeness to θ (%)	100.0	100.0	100.0	100.0
μ (mm^{-1})	0.409	0.409	0.449	0.447
Maximum/minimum transmissions		0.9227, 0.9047		0.9566, 0.8964
Data/restraints/parameters	8970/0/572	8397/0/526	11543/4/953	5769/0/470
R_1[a] [$I > 2.0\sigma(I)$]	0.0403	0.0700	0.0890	0.0972
wR_2[b] (all data)	0.1061	0.1545	0.1548	0.1911
R_{int}	0.0335	0.0723	0.0951	0.0842
GOF on F^2	1.033	1.117	1.106	1.264

[a] $R_1 = \sum \|F_o\| - |F_c\|/\sum \|F_o\|$.
[b] $wR_2 = \{\sum w(F_o^2 - F_c^2)^2 / \sum w(F_o^2)^2\}^{1/2}$.

3. Experimental

3.1. General procedures

All manipulations were carried out on a standard high vacuum line or in a drybox under the atmosphere of nitrogen. Unless noted otherwise, reagents were used as obtained from the commercial suppliers. The solvents were dried and freshly distilled prior to use. $Cp_2Zr\{(\mu-H)_2BHCH_3\}_2$ [8], $Cp_2Zr\{(\mu-H)_2BHPh\}_2 \cdot (1/2$ toluene) [14], and $Cp_2ZrH\{(\mu-H)_2BHPh\}$ [14] were prepared according to the literature methods. Elemental analyses were recorded on a Hitachi 270–30 spectrometer. Proton spectra (δ(TMS) 0.00 ppm) were recorded on a Bruker Avance DPX300 spectrometer operating at 300.132 MHz. ^{11}B spectra (externally referenced to $BF_3 \cdot OEt_2$ (δ 0.00 ppm)) were recorded on a Varian Unity Inova 600 operating at 192.481 MHz, or on a Bruker Avance DPX300 spectrometer operating at 96.294 MHz. Infrared spectra were recorded on a Jasco FT/IR-460 Plus spectrometer with 2 cm^{-1} resolution.

3.2. X-ray crystal structure determination

Suitable single crystals were mounted and sealed inside glass fibers under nitrogen. Crystallographic data collec-

tions were carried out on a Nonius KappaCCD diffractometer with graphite monochromated Mo Kα radiation ($\lambda = 0.71073$ Å) at 150(1) K. Cell parameters were retrieved and refined using DENZO-SMN [20] software on all reflections. Data reduction was performed using the DENZO-SMN [20] software. An empirical absorption correction was based on the symmetry-equivalent reflections and was applied to the data using the SORTAV [21] program. Structure analysis was performed using SHELXTL program on a personal computer. Structures were solved using the SHELXS-97 [22] program and refined using SHELXL-97 [23] program by full-matrix least-squares on F^2 values. All non-hydrogen atoms were refined anisotropically. Hydrogen atoms attached to the borons were located from the d-Fourier map and refined isotropically. Hydrogen atoms attached to the carbons were fixed at calculated positions and refined using a riding mode. Detailed crystallographic data are listed in Table 3.

3.3. Preparation of complexes

3.3.1. $Cp_2ZrH\{(\mu-H)_2BHCH_3\}$ (1)

$Cp_2Zr\{(\mu-H)_2BHCH_3\}_2$ (922.1 mg, 3.3 mmol) and about 15 mL of diethyl ether were added into a flask. After degassing, a 0.46 mL (3.3 mmol) of $N(C_2H_5)_3$ was trans-

Table 4
Selected interatomic distances (Å) and bond angles (°) for [Cp$_2$Zr(OEt$_2$){(μ-H)$_2$BHPh}][HB(C$_6$F$_5$)$_3$] (3)

Bond lengths

av Zr–C(7-11)[a]	2.49 [1]	Zr–H(1B)	2.10(5)
av Zr–C(12-16)[a]	2.497 [4]	B(1)–H(1C)	1.13(5)
Zr–B(1)	2.561(5)	B(1)–H(1B)	1.20(5)
Zr–O(1)	2.263(3)	B(1)–H(1A)	1.28(4)
Zr–H(1A)	1.92(4)		

Angles

H(1A)–Zr–H(1B)	55.3(19)	H(1B)–B(1)–C(1)	111(2)
H(1C)–B(1)–H(1B)	114(3)	H(1A)–B(1)–C(1)	110(2)
H(1C)–B(1)–H(1A)	108(3)	C(19)–O(1)–C(17)	112.1(3)
H(1B)–B(1)–H(1A)	98(3)	C(19)–O(1)–Zr	119.3(2)
H(1C)–B(1)–C(1)	114(3)	C(17)–O(1)–Zr	125.4(2)

[a] The standard derivation (σ_l) for the average bond length of Zr–C is calculated according to the equations [19]

$$\langle l \rangle = \Sigma_m l_m / m,$$

$$\sigma_l = [\Sigma_m (l_m - \langle l \rangle)^2 / (m(m-1))]^{1/2},$$

where $\langle l \rangle$ is the mean length, l_m is the length of the *m*th bond, and *m* is the number of bonds.

Table 5
Selected interatomic distances (Å) and bond angles (°) for [Cp$_2$Zr(OEt$_2$){(μ-H)$_2$BHCH$_3$}][HB(C$_6$F$_5$)$_3$] (4)

Bond lengths

av Zr(1)–C(6–10)[a]	2.47 [1]	av Zr(2)–C(21–25)[a]	2.479 [7]
av Zr(1)–C(11–15)[a]	2.48 [1]	av Zr(2)–C(26–30)[a]	2.47 [1]
Zr(1)–B(1)	2.514(12)	Zr(2)–B(2)	2.575(12)
Zr(1)–O(1)	2.243(5)	Zr(2)–O(2)	2.261(5)
Zr(1)–H(1A)	1.95(8)	Zr(2)–H(2A)	1.92(9)
Zr(1)–H(1B)	1.97(8)	Zr(2)–H(2B)	1.95(9)
B(1)–H(1B)	1.13(9)	B(2)–H(2C)	1.19(9)
B(1)–H(1A)	1.17(8)	B(2)–H(2A)	1.201(10)
B(1)–H(1C)	1.27(8)	B(2)–H(2B)	1.204(11)

Angles

H(1A)–Zr(1)–H(1B)	53(3)	H(2A)–Zr(2)–H(2B)	51.4(15)
H(1B)–B(1)–H(1A)	98(6)	H(2C)–B(2)–H(2A)	92(6)
H(1B)–B(1)–H(1C)	98(6)	H(2C)–B(2)–H(2B)	96(6)
H(1A)–B(1)–H(1C)	100(5)	H(2A)–B(2)–H(2B)	89(6)
H(1B)–B(1)–C(1)	113(4)	H(2C)–B(2)–C(16)	132(5)
H(1A)–B(1)–C(1)	122(4)	H(2A)–B(2)–C(16)	126(5)
H(1C)–B(1)–C(1)	121(4)	H(2B)–B(2)–C(16)	111(5)
H(1A)–Zr(1)–O(1)	72(2)	H(2A)–Zr(2)–O(2)	125.3(11)
H(1B)–Zr(1)–O(1)	123(3)	H(2B)–Zr(2)–O(2)	74.4(13)
C(4)–O(1)–C(2)	112.6(7)	C(19)–O(2)–C(17)	112.7(5)
C(4)–O(1)–Zr(1)	125.7(5)	C(19)–O(2)–Zr(2)	123.5(4)
C(2)–O(1)–Zr(1)	119.9(5)	C(17)–O(2)–Zr(2)	121.8(4)

[a] The standard derivation (σ_l) for the average bond length of Zr–C is calculated according to the equations [19]

$$\langle l \rangle = \Sigma_m l_m / m,$$

$$\sigma_l = [\Sigma_m (l_m - \langle l \rangle)^2 / (m(m-1))]^{1/2},$$

where $\langle l \rangle$ is the mean length, l_m is the length of the *m*th bond, and *m* is the number of bonds.

Table 6
Selected interatomic distances (Å) and bond angles (°) for [Cp$_2$Zr(OEt$_2$){(μ-H)$_2$BH$_2$}][HB(C$_6$F$_5$)$_3$] (5)

Bond lengths

av Zr–C(1–5)[a]	2.48 [1]	Zr–H(1B)	2.00(10)
av Zr–C(6-10)[a]	2.50 [1]	B(1)–H(1D)	1.04(10)
Zr–B(1)	2.531(13)	B(1)–H(1B)	1.17(10)
Zr–O(1)	2.253(5)	B(1)–H(1C)	1.24(10)
Zr–H(1A)	1.86(10)	B(1)–H(1A)	1.29(10)

Angles

H(1A)–Zr–H(1B)	56(4)	H(1B)–B(1)–H(1A)	95(6)
H(1D)–B(1)–H(1B)	122(8)	H(1C)–B(1)–H(1A)	104(6)
H(1D)–B(1)–H(1C)	124(7)	C(11)–O(1)–C(13)	113.0(6)
H(1B)–B(1)–H(1C)	105(7)	C(11)–O(1)–Zr	120.7(5)
H(1D)–B(1)–H(1A)	101(7)	C(13)–O(1)–Zr	123.7(5)

[a] The standard derivation (σ_l) for the average bond length of Zr–C is calculated according to the equations [19]

$$\langle l \rangle = \Sigma_m l_m / m,$$

$$\sigma_l = [\Sigma_m (l_m - \langle l \rangle)^2 / (m(m-1))]^{1/2},$$

where $\langle l \rangle$ is the mean length, l_m is the length of the *m*th bond, and *m* is the number of bonds.

under a dynamic vacuum, and the resulting white solid was redissolved in ether and kept at −35 °C until crystallization occurred. Isolation of crystalline material resulted in 696.0 mg of Cp$_2$ZrH{(μ-H)$_2$BHCH$_3$} (84% yield) [9].

3.3.2. Cp$_2$Zr{(μ-H)$_2$B(C$_6$F$_5$)$_2$}$_2$ · (C$_6$H$_6$) (2)

Method 1. In a drybox Cp$_2$Zr{(μ-H)$_2$BHCH$_3$}$_2$ (141.7 mg, 0.5 mmol) and B(C$_6$F$_5$)$_3$ (516.0 mg, 1.0 mmol) were placed into a flask. The flask was evacuated, and approximately 20 mL of benzene was transferred into the flask at −78 °C. The flask was gradually warmed to room temperature and kept at room temperature overnight. Fine crystals of Cp$_2$Zr{(μ-H)$_2$B(C$_6$F$_5$)$_2$}$_2$ · (C$_6$H$_6$) [10] formed. The solution was removed, and the crystals were washed with two portions of 5 mL of benzene and dried under vacuum. The title compound was isolated as fine crystals (320.0 mg, 64% yield).

Method 2. Using Cp$_2$Zr{(μ-H)$_2$BHPh}$_2$ · (1/2 toluene) (225.0 mg, 0.50 mmol), B(C$_6$F$_5$)$_3$ (511.2 mg, 1.0 mmol) and 25 mL of benzene in a procedure similar to the one described in method 1 furnished 260.0 mg (52% yield) of fine crystals of the title compound.

Method 3. Using Cp$_2$ZrH{(μ-H)$_2$BHCH$_3$} (84.0 mg, 0.33 mmol), B(C$_6$F$_5$)$_3$ (510.0 mg, 1.0 mmol) and 10 mL of benzene in a procedure similar to the one described in method 1 yielded 160.0 mg (49% yield) of fine crystals of the title compound.

Method 4. Using Cp$_2$ZrH{(μ-H)$_2$BHPh} (157.0 mg, 0.5 mmol), B(C$_6$F$_5$)$_3$ (770.0 mg, 1.5 mmol) and 10 mL of benzene in a procedure similar to

ferred into the flask at −78 °C. The flask was gradually warmed to room temperature resulting in a clear solution. After stirring for 4 h, the volatile species were removed

the one described in method 1 afforded 234.0 mg (47% yield) of fine crystals of the title compound. ^{11}B NMR (benzene): δ −13.4 ppm (t, J_{B-H} = 64 Hz). ^{1}H NMR (C_6D_6): δ 5.38 (s, 10H, Cp), 0.40 ppm (br, q, 4H, μ-H). IR(KBr): 3130(br, vw), 2357(br, vw), 2318(br, vw), 2183(br, w), 2112(br, w), 2027(br, vw), 1643(m), 1514(s), 1475(vs), 1379(vw), 1333(w), 1288(m), 1261(m), 1112(m), 1097(m), 1012(vw), 989(vw), 955(m), 920(vw), 885(w), 858(vw), 827(m), 756(vw), 720(vw), 687(w), 625(vw), 606(vw), 563(vw) cm^{-1}. $C_{40}H_{20}B_2F_{20}Zr$: C, 48.36; H, 2.03. Found: C, 48.44; H, 2.03%.

3.3.3. [Cp₂Zr(OEt₂){(μ-H)₂BHPh}][HB(C₆F₅)₃] (3)

In a drybox a 50 mL flask was charged with 101.7 mg (0.32 mmol) of Cp₂ZrH{(μ-H)₂BHPh} and 166.2 mg (0.32 mmol) of B(C₆F₅)₃. The flask was evacuated, and about 10 mL of the diethyl ether was condensed into it at −78 °C. The flask was warmed to room temperature followed by stirring of the reaction mixture for 4 h. A white solid was obtained after removal of the solvent. The solid was redissolved in diethyl ether and layered with hexane. The title compound was obtained as colorless crystals (190 mg, 66% yield). ^{11}B NMR (d_8-THF): δ 11.90 (br), −26.16 ppm (d, J_{B-H} = 93 Hz). ^{11}B NMR (ether): δ 13.75 (br), −25.43 ppm (d, J_{B-H} = 90 Hz). ^{1}H NMR (d_8-THF): δ 7.39–7.20 (m, 5H, Ph), 6.70 (s, 10H, Cp), 3.74 (br, q, 1H, HB), 3.39 (q, 4H, ether), 1.20 (br, 3H, H₃B), 1.12 ppm (t, 6H, ether). IR(KBr): 3072(vw), 3033 (vw), 2999(vw), 2976(w), 2931(w), 2900(w), 2870(w), 2816(vw), 2345(s), 2220(w), 2195(s), 2148(vw), 1942(vs), 1840(vs), 1736(vw), 1639(vw), 1483(s), 1450(w), 1417 (w), 1383(vw), 1369(vw), 1340(vw), 1288(vw), 1234(vw), 1188(w), 1122(s), 1028(vw), 947(m), 935(w), 858(w), 796(vw), 637(vw), 611(vw), 578(vw), 565(vw), 517 (w), 494(vw), 472(vw), 409(vw) cm^{-1}. Anal. Calc. for $C_{38}H_{29}B_2F_{15}OZr$: C, 50.74; H, 3.25. Found: C, 50.60; H, 3.24%.

3.3.4. [Cp₂Zr(OEt₂){(μ-H)₂BHCH₃}][HB(C₆F₅)₃] (4)

Cp₂Zr{(μ-H)₂BHCH₃}₂ (140.2 mg, 0.5 mmol) and B(C₆F₅)₃ (257.0 mg, 0.5 mmol) were placed into a reaction flask. The flask was evacuated, and about 10 mL of diethyl ether was transferred into the flask at −78 °C. The solution was gradually warmed to room temperature and stirred until it became clear. Crystals of [Cp₂Zr(OEt₂){(μ-H)₂BHCH₃}][HB(C₆F₅)₃] grew slowly from this solution. After standing at room temperature overnight, the ether solution was removed, and the crystals were washed twice with 10 mL portions of cold ether and dried under vacuum. The title compound was obtained as colorless crystals (290.0 mg, 69.3% yield). ^{11}B NMR (THF): δ 13.34 (br), −26.57 ppm (d, J_{B-H} = 93 Hz). ^{11}B NMR (ether): δ 15.77 (br, q), −25.36 ppm (d, J_{B-H} = 90 Hz). ^{1}H NMR (d_8-

THF): δ 6.70 (s, 10H, Cp), 3.75 (br, q, 1H, HB), 3.39 (q, 4H, ether), 1.12 (t, 6H, ether), 0.47 (br, q, J_{H-H} = 3.9 Hz, 3H, CH₃), and 0.65 ppm (br, 3H, H₃B). IR(KBr): 3118(w), 2983(w), 2943(w), 2904(vw), 2870(vw), 2420(w), 2360(w), 2337(w), 2287(vw), 2027(vw), 1957(vw), 1874(vw), 1639(m), 1603(vw), 1554(vw), 1510(s), 1464(vs), 1412(w), 1392(w), 1377(m), 1302(vw), 1273(m), 1219(vw), 1188(vw), 1113(m), 1103(m), 1068(m), 1016(w), 991(w), 966(s), 908(w), 881(vw), 827(m), 789(vw), 764(m), 725(vw), 660(w), 648(w), 602(vw), 567(vw), and 409(w) cm^{-1}. Anal. Calc. for $C_{33}H_{27}B_2F_{15}OZr$: C, 47.33; H, 3.25. Found: C, 46.94; H, 3.31%.

3.3.5. [Cp₂Zr(OEt₂){(μ-H)₂BH₂}][HB(C₆F₅)₃] (5)

Using Cp₂Zr{(μ-H)₂BHPh}₂ · (1/2 toluene) (225.0 mg, 0.50 mmol), B(C₆F₅)₃ (256.0 mg,0.50 mmol) and 15 mL of diethyl ether in a procedure is similar to the one describing the preparation of **4** afforded 360.0 mg (87.4% yield) of the title compound as colorless crystals. ^{11}B NMR (THF): δ 2.08 (br, quintet), −26.00 ppm (d, J_{B-H} = 92 Hz). ^{11}B NMR (ether): δ 4.33 (br), −25.14 ppm (d, J_{B-H} = 90 Hz). ^{1}H NMR (d_8-THF): δ 6.71 (s, 10H, Cp), 3.72 (br, q, 1H, HB), 3.39 (q, 4H, ether), 1.12 (t, 6H, ether), 0.85 ppm (br, 3H, H₃B). IR(KBr): 3119(br, w), 2986(vw), 2486(w), 2426(m), 2376(w), 2270(vw), 2141(w), 2071(vw), 1954(w), 1639(m), 1603(vw), 1549(vw), 1510(s), 1460(vs), 1392 (w), 1377(w), 1344(m), 1317(w), 1273(m), 1184(vw), 1134(m), 1114(m), 1103(m), 1070(m), 1014(m), 991 (w), 966(s), 906(w), 881(vw), 831(m), 796(vw), 762(m), 725(vw), 658(w), 650(w), 603(vw), 569(vw), 518(vw), 469(vw), 446(vw), 423(vw) cm^{-1}. Anal. Calc. for $C_{32}H_{25}B_2F_{15}OZr$: C, 46.58; H, 3.06. Found: C, 46.49; H, 3.01%.

3.3.6. NMR study of the reaction of Cp₂Zr{(μ-H)₂-BHPh}₂ · (1/2 toluene) with B(C₆F₅)₃ in diethyl ether

Cp₂Zr{(μ-H)₂BHPh}₂ · (1/2 toluene) (10.0 mg, 0.022 mmol) and B(C₆F₅)₃ (11.4 mg, 0.022 mmol) were placed into an NMR tube. After degassing, the diethyl ether was transferred into the tube, and the tube was sealed. After warming it to room temperature a clear solution formed that was monitored by ^{11}B NMR.

3.3.7. Blank experiment: [Cp₂Zr(OC₄H₁₀){(μ-H)₂-BHPh}][HB(C₆F₅)₃] and Cp₂Zr{(μ-H)₂BHPh}₂ · (1/2 toluene) in diethyl ether

A reaction flask was charged with 50.0 mg of [Cp₂Zr(OEt₂){(μ-H)₂BHPh}][HB(C₆F₅)₃] and 10.1 mg of Cp₂Zr{(μ-H)₂BHPh}₂ · (1/2 toluene). After degassing, about 5 mL of diethyl ether was transferred into the flask at −78 °C. The flask was warmed to room temperature followed by stirring for 30 h. The solvent was removed, and the resulting solid was dissolved in THF. The ^{11}B NMR of the solution was acquired. The starting material Cp₂Zr{(μ-H)₂BHPh}₂ and a partial decomposition of [Cp₂Zr(OEt₂){(μ-H)₂BHPh}][HB(C₆F₅)₃] with formation of [Cp₂Zr(OEt)(OEt₂)][HB(C₆F₅)₃] were observed, how-

ever, the characteristic signal of the cation $[Cp_2Zr(OEt_2)\{(\mu\text{-}H)_2BH_2\}]^+$ was not found.

3.3.8. Preparation of $[Cp_2Zr(OEt)(OEt_2)][HB(C_6F_5)_3]$ (6)

Method 1. In a drybox a reaction flask was charged with 225.0 mg of $Cp_2Zr\{(\mu\text{-}H)_2BHPh\}_2 \cdot (1/2$ toluene) (0.5 mmol) and 514.0 mg of $B(C_6F_5)_3$ (1.0 mmol). The flask was evacuated, and about 10 mL of diethyl ether was transferred into the flask at $-78\ ^\circ C$. The flask was gradually warmed to room temperature, and the reaction mixture was stirred until a clear solution was formed. In the drybox the solvent was allowed to evaporate slowly from the solution at room temperature yielding 307.0 mg (72% yield) of crystalline title compound.

Method 2. $Cp_2Zr\{(\mu\text{-}H)_2BHCH_3\}_2$ (70.0 mg, 0.25 mmol), 256.0 mg (0.5 mmol) of $B(C_6F_5)_3$, and 10 mL of diethyl ether transferred into the flask at $-78\ ^\circ C$ were allowed to warm up to room temperature resulting in a clear solution. The solution was stood aside at room temperature overnight for crystallization. The crystals were filtered off and washed twice with 3 mL portions of diethyl ether. A total of 95.0 mg of crystals was obtained. By ^{11}B and ^{1}H NMR spectroscopy they were identified as a mixture of $[Cp_2Zr(OEt_2)\{(\mu\text{-}H)_2BHCH_3\}][HB(C_6F_5)_3]$ and $[Cp_2Zr(OEt)(OEt_2)][HB(C_6F_5)_3]$.

Method 3. $Cp_2ZrH\{(\mu\text{-}H)_2BHCH_3\}$ (126.2 mg, 0.5 mmol), $B(C_6F_5)_3$ (256.0 mg, 0.5 mmol) and 10 mL of diethyl ether were used. The procedure was similar to the one described in method 1. After standing at room temperature overnight, the solution turned pink. This solution was concentrated and kept at $-35\ ^\circ C$ for crystallization. Pink-colored crystals (130 mg, 30.5%) were isolated. ^{11}B NMR spectrum confirmed the formation of $[Cp_2Zr(OEt)(OEt_2)][HB(C_6F_5)_3]$.

3.3.9. NMR study of $Cp_2ZrH\{(\mu\text{-}H)_2BHCH_3\}$ with of $B(C_6F_5)_3$ in diethyl ether

$Cp_2ZrH\{(\mu\text{-}H)_2BHCH_3\}$ (6.2 mg, 0.025 mmol) and $B(C_6F_5)_3$ (12.6 mg, 0.025 mmol) were added into a NMR tube. The tube was degassed followed by transfer of about 0.4 mL diethyl ether onto the reagents at $-78\ ^\circ C$. The tube was gradually warmed to room temperature. During the warm-up process, the reaction occurred, and an unidentified gas evolved. The tube was sealed, and the boron spectra were acquired.

Acknowledgment

Appendix A. Supplementary material

CCDC 624286, 624285, 624289, 624287, and 624288, contain the supplementary crystallographic data for **2**, **3**, **4**, **5**, and **6**. The data can be obtained free of charge via htpp://www.ccdc.cam.ac.uk/conts/retrieving.html, or from the Cambridge Crystallographic Data Centre, 12 Union Road, Cambridge CB2 1EZ, UK; fax: (+44) 1223-336-033; or e-mail: deposit@ccdc.cam.ac.uk. Supplementary data associated with this article can be found, in the online version, at doi:10.1016/j.jorganchem.2007.02.031.

References

[1] (a) R.F. Jordan, Chemistry of Cationic Dicyclopentadienyl Group 4 Metal-Alkyl Complexes, In: Advances in Organometallic Chemistry, 32, Academic Press, New York, 1991, p. 325;
(b) H. Sinn, W. Kaminsky, Adv. Organomet. Chem. 18 (1980) 99;
(c) A.S. Guram, R.F. Jordan, Cationic Organozirconium and Organohafnium Complexes, in: E.W. Abel, F.G.A. Stone, G. Wilkinson (Eds.), Comprehensive Organometallic Chemistry, II, vol. 4, Elsevier Science, Ltd., New York, 1995 (Chapter 12).
[2] (a) R. Taube, L. Krukowka, J. Organomet. Chem. C9 (1988) 347;
(b) Z. Lin, J.-F. Le Marechal, M. Sabat, T.J. Marks, J. Am. Chem. Soc. 109 (1987) 4127;
(c) J.J.W. Eshuis, Y.Y. Tan, J.H. Teuben, J. Renkema, J. Mol. Catal. 62 (1990) 277;
(d) M. Bochmann, A.J. Jagger, L.M. Wilson, M.B. Hursthouse, M. Motevalli, Polyhedron 8 (1989) 1838;
(e) R.F. Jordan, W.E. Dasher, S.F. Echols, J. Am. Chem. Soc. 108 (1986) 1718;
(f) E.Y.-X. Chen, T.J. Marks, Chem. Rev. 100 (2000) 1391;
(g) A.L. Mckinbht, R.M. Waymouth, Chem. Rev. 98 (1998) 2587.
[3] R.F. Jordan, P.K. Bradley, R.E. LaPointe, D.F. Taylor, New J. Chem. 14 (1990) 505.
[4] (a) X. Yang, C.L. Sterm, T.J. Marks, J. Am. Chem. Soc. 116 (1994) 10015;
(b) X. Yang, C.L. Sterm, T.J. Marks, J. Am. Chem. Soc. 113 (1991) 3623.
[5] (a) F.-C. Liu, J. Liu, E.A. Meyers, S.G. Shore, J. Am. Chem. Soc. 122 (2000) 6106;
(b) S.G. Shore, F.-C. Liu, Cationic Metallocenes Derived from Cyclic Organohydroborate Metallocene Complexes, in: M.G. Davidson, A.K. Hughes, T.B. Marder, K. Wade (Eds.), Contemporary Boron Chemistry, The Royal Society of Chemistry, London, 2000, pp. 28–35.
[6] C.E. Plečnik, F.-C. Liu, S. Liu, J. Liu, E.A. Meyers, S.G. Shore, Organometallics 20 (2001) 3599.
[7] S. Liu, F.-C. Liu, G. Renkes, S.G. Shore, Organometallics 20 (2001) 5717.
[8] F.-C. Liu, K.-Y. Chen, J.-H. Chen, G.-H. Lee, S.-M. Peng, Inorg. Chem. 42 (2003) 1758.
[9] W.K. Kot, N.M. Edelstein, A. Zalkin, Inorg. Chem. 26 (1987) 1339.
[10] (a) R.E.v.H. Spence, W.E. Piers, Y. Sun, M. Parvez, L.R. MacGillivray, M.J. Zaworotko, Organometallics 17 (1998) 2459;
(b) R.E.v.H. Spence, D.J. Parks, W.E. Piers, M.-A. MacDonald, M.J. Zaworotko, S.J. Rettig, Angew. Chem., Int. Ed. Engl. 34 (1995) 1230.
[11] H.I. Schlesinger, H.C. Brown, L. Horvitz, A.C. Bond, L.D. Tuck, A.C. Walker, J. Am. Chem. Soc. 75 (1953) 222.
[12] T.J. Marks, J.R. Kolb, J. Am. Chem. Soc. 97 (1975) 27.

[13] X. Chen, F.-C. Liu, C.E. Plečnik, S. Liu, B. Du, E.A. Meyers, S.G. Shore, Organometallics 23 (2004) 2100.

[14] F.-C. Liu, J.-H. Chen, S.-C. Chen, K.-Y. Chen, G.-H. Lee, S.-M. Peng, J. Organomet. Chem. 690 (2005) 291.

[15] R. Choukroun, B. Douziech, B. Donnadieu, Organometallics 16 (1997) 5517.

[16] R.F. Jordan, C.S. Bajgur, R. Willet, B. Scott, J. Am. Chem. Soc. 108 (1986) 7410.

[17] S. Collins, B.E. Koene, R. Ramachandran, N.J. Taylor, Organometallics 10 (1991) 2092.

[18] (a) W.A. Howard, G. Parkin, J. Am. Chem. Soc. 116 (1994) 606;
(b) W.A. Howard, M. Waters, G. Parkin, J. Am. Chem. Soc. 115 (1993) 4917.

[19] G.H. Stout, L.H. Jensen, X-ray Structure Determination, second ed., Wiley, New York, 1989, pp. 406–408.

[20] DENZO-SMN: Z. Otwinowsky, W. Minor, Processing of X-ray Diffraction Data Collected in Oscillation Mode, in: Methods in Enzymology, in: C.W. CarterJr., R.M. Sweet (Eds.), Macromolecular Crystallography, Part A, vol. 276, Academic Press, New York, 1997, pp. 307–326.

[21] (a) R.H. Blessing, Acta Crystallogr., Sect. A 51 (1995) 33;
(b) R.H. Blessing, J. Appl. Crystallogr. 30 (1997) 421.

[22] SHELXS-97: G.M. Sheldrick, Acta Crystallogr., Sec. A 46 (1990) 467.

[23] G.M. Sheldrick, SHELXL-97, University of Göttingen, Göttingen, Germany, 1997.